Drug-loaded Polymeric Spherical Nucleic Acids: Enhancing Colloidal Stability and Cellular Uptake of Polymeric Nanoparticles through DNA Surface-functionalization

Resham J. Banga[a], **Sai Archana Krovi**[b,d], **Suguna P Narayan**[c], **Anthony J. Sprangers**[c], **Guoliang Liu**[d,e], **Chad A. Mirkin**[d,f], and **SonBinh T. Nguyen**[d,f,*]

[a]Department of Chemical and Biological Engineering, Northwestern University, 2145 Sheridan Road, Evanston, Illinois-60208-3113, USA

[c]Department of Biomedical Engineering, Northwestern University, 2145 Sheridan Road, Evanston, Illinois-60208-3113, USA
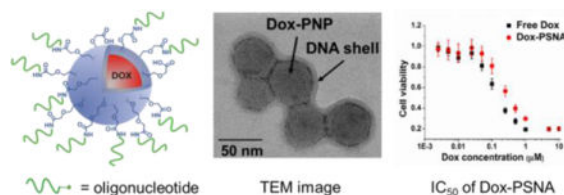
[d]Department of Chemistry, Northwestern University, 2145 Sheridan Road, Evanston, Illinois-60208-3113, USA

[f]International Institute of Nanotechnology, Northwestern University, 2145 Sheridan Road, Evanston, Illinois-60208-3113, USA

Abstract

Small-sized (~65 nm) doxorubicin (Dox)-loaded polymeric nanoparticles (PNPs) were modified with oligonucleotides to form colloidally stable Dox-loaded polymeric spherical nucleic acid (Dox-PSNA) nanostructures in biological media. The nucleic acid shell facilitates the cellular uptake of Dox-PSNA, resulting in *in-vitro* cytotoxicity against SKOV3 cancer cells.

TOC figure

[*]Corresponding Author: stn@northwestern.edu.
[b]Current address: UNC Eshelman School of Pharmacy, University of North Carolina at Chapel Hill, 301 Pharmacy Lane Beard Hall, Chapel Hill, North Carolina 27599;
[e]Current address: Department of Chemistry, Virginia Tech, Blacksburg, Virginia 24061, USA;

Author Manuscript

Author Manuscript

Author Manuscript

Author Manuscript

Keywords

Drug-loaded nanoparticles; polymeric nanoparticles; spherical nucleic acids; doxorubicin; ring-opening metathesis polymerization

---

Polymeric nanoparticles (PNPs) prepared from amphiphilic ROMP block copolymers (ROMP = ring-opening metathesis polymerization) represent a versatile class of multifunctional nanoconstructs for biodetection,[1,2] imaging,[3] and drug delivery.[4,5] In particular, the ease with which these nanoparticles can be surface-functionalized[2] with a multitude of biologically active entities[2,6] has shown promise in many drug delivery applications.[5,7,8] Previously, we reported that ROMP-based doxorubicin-loaded PNPs can be modified with cationic surface moieties post-assembly to improve their stability in buffered media and *in vitro* cellular uptake.[7] However, the large diameters of these particles (~100–200 nm) may limit their cellular uptake[9] and tumor penetration when delivered *in vivo*.[10,11] Thus, we set out to improve the bioavailability of the doxorubicin-loaded PNP platform by reducing nanoparticle size and covalently modifying the surface with negatively charged oligonucleotides, which have been shown to promote higher cellular uptake.[12] Since sub-100 nm-sized nanoparticles have been shown to exhibit increased cellular uptake and better penetration into tumor tissue,[13,14] these two modifications may allow for extended stability under physiologically relevant conditions and should enhance overall efficacy for *in vivo* applications.

The high-density surface modification of nanoparticles with oligonucleotides results in a three-dimensional architecture known as a spherical nucleic acid (SNA).[12] The dense oligonucleotide shells in SNAs have been shown to stabilize a broad range of nanoparticle cores–from inorganic Au,[15] Ag,[16] and silica[17] ones to organic structures such as ultra-small liposomes,[18] proteins,[19] and polymers[20,21]–under physiological conditions via electrostatic repulsion.[18] The SNA architecture also promotes superior cellular internalization for the nanoparticle cores over PEG-functionalized analogs[22] and linear nucleic acids,[23] given its ability to bind to cellular membrane-bound scavenger receptors,[23] which facilitate cellular internalization via endosomal pathways.[12,24] As a result, SNA structures have been utilized in a wide variety of applications spanning biodetection,[22] gene regulation[25], drug delivery,[26–28] and immunomodulation.[12,29] By covalently modifying small (sub-100 nm) doxorubicin-loaded PNPs with oligonucleotides (Scheme 1), we show herein that the resulting doxorubicin-loaded polymeric SNA (Dox-PSNA) structures are stable under physiologically relevant conditions, are capable of active cellular internalization, and exhibit cytotoxicity with respect to SKOV-3 ovarian cancer cells. While the potency of these Dox-PSNA nanoparticles is comparable to that of the free drug, they should not be prone to the renal clearance issues that plague small molecules.[30]

MATERIALS AND METHODS

Materials and Instrumentation

Please see SI, Section S1

Synthesis of block copolymer 2_{15}-*b*-1_{15}

In an inert-atmosphere glovebox, monomer **2** (25 mg, 45.2 μmol; see SI, Section S2 for the synthesis of monomer **2**) was dissolved in an anhydrous mixture of $CHCl_3$/MeOH (9:1 v/v, 1 mL) in a 20 mL scintillation vial equipped with a magnetic stir bar. A stock solution of Grubbs' first-generation catalyst (5 mg) in $CHCl_3$/MeOH (9:1 v/v, 5 mL) was prepared, a portion of which (2.48 mL, 3.01 μmol) was added to the vial containing the solution of monomer **2** under vigorous stirring. The resulting reaction mixture was stirred for 45 min at room temperature, at which time an aliquot (100 μL) was removed and quenched with excess ethyl vinyl ether. A portion of this quenched aliquot was evaporated to dryness, redissolved in $CDCl_3$, and analyzed by ^1H NMR spectroscopy, which indicated complete consumption of the monomer. The remaining portion was evaporated to dryness, dissolved in HPLC-grade THF, and subjected to GPC analysis (M_n = 9000 (theoretical M_n = 8000), PDI = 1.13).

Immediately after aliquot removal, a solution of monomer **1** (see SI, Section S1, 30.7 mg, 45.2 μmol) in $CHCl_3$/MeOH (9:1 v/v, 1 mL) was added to the reaction vial and the resulting polymerization mixture was stirred for an additional 45 min before being terminated with the addition of ethyl vinyl ether (1 mL). The reaction mixture was added quickly into vigorously stirred cold (−10 °C) pentanes (200 mL), and the resulting precipitate was isolated *via* vacuum-filtration and washed thoroughly with fresh pentanes to afford the product copolymer quantitatively as a red solid. See the SI for the ^1H NMR spectrum, Section S3). Due to the lack of complete polymerization of monomer **1** when being initiated as the first block,[7,31] we did not attempt to synthesize the reverse block copolymer 1_{15}-*b*-2_{15}.

To maximize the number of chemical handles that can subsequently be used for surface functionalization of the PNPs, we employed a block copolymer with an equimolar ratio of monomers **2**:**1**, while keeping the PNP diameter < 100 nm.

General procedure for the preparation of PNPs in the 60–75 nm size range

An aqueous suspension of the polymer nanoparticles was prepared by dialysis following a modification of the published procedure.[7] An aliquot (2.5 mL) of a stock solution of block copolymer 2_{15}-*b*-1_{15} (0.01 wt %) in DMSO was transferred to a 4 mL scintillation vial and stirred vigorously. Ultrapure deionized water was added to this stirring copolymer solution at a rate of 1 drop (50 μL, 1.75 wt %) every 1 s using a 20–100 μL micro-pipette until the mixture contained 18 wt % water. The resulting cloudy mixture was placed in a 3 mL dialysis cassette and dialyzed against ultrapure deionized water (500 mL), with the dialate changed every 2 h. Complete absence of DMSO in the dialysate after 48 h was verified by UV-vis spectroscopy as indicated by the disappearance of the UV cut-off for DMSO at 268 nm.

Characterization of PNPs derived from block copolymer 2_{15}-*b*-1_{15}

DLS analysis of the final PNP aqueous suspension derived from block copolymer 2_{15}-*b*-1_{15} revealed relatively monodisperse PNPs with an average D_H = 63 ± 7 nm and a PDI = 0.11 (Figure 1B). TEM analysis indicated a uniform size distribution for the PNPs in the solid-

state, with an average diameter of ~65 nm (Figure 1C) that is consistent with the DLS data. The zeta potential of these PNPs was determined to be -6.83 ± 0.5 mV. The average concentration of PNP particles is $\sim 1 \times 10^{10}$ particles/mL, as determined by NTA. The doxorubicin loading for the PNPs is 64 wt %, as calculated based on the doxorubicin wt% in the 2_{15}-b-1_{15} copolymer.

DNA functionalization of doxorubicin-loaded PNPs and characterization data

In a 1.5 mL safe-lock Eppendorf tube, solutions of N-(3-dimethylaminopropyl)-N'-ethylcarbodiimide hydrochloride (EDC•HCl, final concentration in reaction solution = 5 μM) and N-hydroxysulfosuccinimide (sulfo-NHS, final concentration in reaction solution = 7.5 μM) in ultrapure deionized water were added to an aliquot (1 mL) of the carboxy-functionalized PNP suspension (1×10^{10} particles/mL, ~125,000 carboxylate groups) derived from the desired block copolymer. The reaction mixture was agitated (1000 rpm) on a multi-therm platform shaker (Benchmark Scientific, Inc., South Plainfield, NJ, USA) for 5 min at room temperature. A freshly prepared aliquot of 3′-amino-terminated oligonucleotides (100 μL of a 10 μM solution) was then added to the reaction mixture, and the resulting mixture was covered with aluminum foil and agitated on a multi-therm platform shaker for 4 h at room temperature.

To increase the density of oligonucleotide packing on the PNP surface, EDC and NHS solutions (to 5 μM and 7.5 μM final concentrations, respectively, assuming that all the initially added reagents have been consumed/decomposed) were added to the PNP solution, and the resulting mixture was subjected to a salt-aging process.[32] Aliquots of NaCl (8 μL of a 5 M solution to attain a final [NaCl] = 50 mM) were added to the reaction mixture every 30 min, and the Eppendorf tube was sonicated for 15 s (Branson 2510 ultrasonic cleaner, Branson Ultrasonics, Danbury, CT, USA) after each salt addition. Upon reaching a total NaCl concentration of 300 mM, the reaction mixture was agitated on a multi-therm platform shaker for an additional 12 h at room temperature. The resulting PSNAs were then purified using size-exclusion chromatography (Sepharose CL-4B, Sigma Aldrich). The average concentration of PSNA particles was $\sim 10^9$/mL, as determined by NTA.

Characterization of oligonucleotides-conjugated doxorubicin-loaded PNPs

DLS analysis of the final DNA-functionalized PNP aqueous suspension derived from block copolymer 3_{15}-b-5_{15} revealed relatively monodisperse PNPs with an average $D_H = 88 \pm 3$ nm and a PDI = 0.13. The zeta potential of the oligonucleotide-modified PNPs was determined to be -31.2 ± 3.2, indicating that negatively charged oligonucleotides are conjugated to the PNP surface. For TEM analysis, the PNPs were pre-stained with uranyl acetate solution (10 μL, 2% w/v).

Quantification of oligonucleotides strands on the surface of PSNAs

To assess the degree of oligonucleotide surface modification, an aliquot (20 μL) of the purified Cy5-oligonucleotide-modified PNPs was added to DMSO solution and placed on a multi-therm shaker for 2 h at 37 °C to dissolve the PSNAs. An aliquot (50 μL) of the resulting solution was further mixed with DMSO (final volume = 200 μL), and its fluorescence at the emission wavelength of Cy5 ($\lambda_{ex} = 649$ nm, $\lambda_{em} = 670$ nm) was

recorded using a Synergy HT multi-mode microplate reader (BioTek, Winooski, VT, USA). This fluorescence was compared against a calibration curve constructed from absorbance values for solutions of the Cy5-labeled oligonucleotides in DMSO (concentrations = 0, 0.1, 0.25, 0.5,1, 2.5, 5 μM). From this analysis and the number of PSNA nanoparticles in solution (obtained from NTA), each cholesterol-containing PSNA particle was estimated to have ~1900 oligonucleotides strands and each doxorubicin-loaded PSNA particle was estimated to have ~1200 oligonucleotides strands. The doxorubicin loading is 63.8 wt %, as calculated based on the doxubicin wt % in the $2_{15}\text{-}b\text{-}1_{15}$ copolymer and the total weight of the DNA, assuming an average density of 1 for the whole construct.

Stability study of PNPs and PSNAs

Two separate aliquots of the doxorubicin-containing PNPs and PSNAs (500 μL) were transferred to a 1.5 mL safe-lock Eppendorf tube and centrifuged for 30 min at 10K rpm to a solid pellet. The supernatant was removed and the PNPs were re-suspended in PBS (500 μL, 10 mM, pH 7.4, 150 mM [NaCl]). As expected, characterization of the PNP suspension in PBS resulted in loss of the original well-defined morphology of the parent PNPs as observed by TEM and DLS. The size of PSNAs was analysed periodically over a two month period using DLS. We note in passing that while single-stranded DNA has been adsorbed to the surface of polymer nanoparticles through non-covalent modification,[33,34] such constructs have not been tested for stability in cell culture media.

Melt Analysis

Melt analysis experiments were carried out using a Cary 5000 UV-vis spectrometer equipped with a programmable heating stage (ThermoFisher Scientific, Carlsbad, CA, USA). Doxorubicin-containing PSNAs functionalized with Melt A strands were prepared as described above. 13 nm Au-core SNAs functionalized with the complementary Melt B strands (Table S1) were prepared following literature protocols.[32] The aggregates were formed by combining these two materials in a 1:1 ratio (total DNA concentration = 1.5 μM, total volume = 1 mL). The aggregates were then subjected to a temperature ramp from 20 to 65 °C (rate of 0.25 °C/min) while the absorbance for the aggregates was continuously monitored at 260 nm.

Cell culture experiments

SKOV-3 cells were purchased from American Tissue Culture Collection (ATCC, Manassas, VA, USA) and grown in McCoy's 5A medium (Invitrogen, Carlsbad, CA, USA) supplemented with 10% heat-inactivated fetal bovine serum, penicillin (100 IU/mL), and streptomycin (50 μg/mL) and maintained at 37 °C with 5% CO_2 as per ATCC instructions. For cellular studies, the cells were plated at 60% confluency 24 h prior to the treatment.

Confocal microscopy of PSNAs

In a typical experiment, SKOV-3 cells were plated on a 35 mm FluoroDish (World Precision Instruments, Saratosa, FL, USA) and incubated for 24 h before being transfected with the appropriate oligonucleotide formulation (final DNA concentration = 0.1 μM). The treated cells were incubated for 24 h before being washed three times with 1× phosphate-buffered

saline (PBS, Invitrogen) and imaged under a Zeiss LSM 510 inverted laser-scanning confocal microscope using Hoechst 33342 as a nuclear stain. The fluorescence excitation for Cy5 was set as 630 nm and emission 650–710 nm. For Z-stack images, the images were collected in different planes with a depth of 0.3 μM.

Cellular uptake experiments

The cellular uptake of the PSNAs was compared to that of the free drug in SKOV3 cells. In preparation for this analysis, the cells were seeded at 60% confluency in a 96 well plate 24 h before treatment with PSNAs and free doxorubicin. The treatments were carried out at 0.1, 0.5, 1, and 2.5 μM of doxorubicin. The cells were then incubated with either free drug or the PSNAs for 24 h before washing three times with $1\times$ PBS. The cells were then detached from the plate surface by exposing to trypsin (20 μL) for 5 mins and fixed using a 4 % para-formaldehyde solution (in $1\times$ PBS). The intracellular delivery of doxorubicin was quantified via flow cytometry on a Guava easyCyte 8HT instrument (Millipore, Billerica, MA, USA) using the doxorubicin channel and normalized based on the intensity of the untreated cells.

Cell viability studies for doxorubicin and Dox-PSNAs

SKOV-3 (ovarian cancer) cells were seeded in 96 well plates at a density of ~5000 cells per well 24 h before the experiment. Cells were incubated with a fixed amount (100 μL) of solution containing either doxorubicin or Dox-PSNAs that were prepared at varying concentrations in OptiMEM (Invitrogen) at 37 °C. After overnight incubation, the media was replaced with regular growth medium (McCoy's 5A supplemented with 10% heat-inactivated fetal bovine serum, penicillin (100 IU/mL), and streptomycin (50 μg/mL)), and the cells were incubated at 37 °C for an additional 48 h. Cell viability was assessed using the alamarBlue® cell viability assay (ThermoFisher Scientific, Carlsbad, CA, USA) according to the manufacturer's recommended protocol. Briefly, 10% alamarBlue® reagent in regular growth medium was added to cells (100 μL per well), and the treated cell plate was incubated at 37 °C for 4 h before being analyzed on a Synergy H4 Multimode Microplate Reader. Fluorescence data at 570 nm were collected and normalized to that for an untreated control. Reported values represent the mean ± standard deviation of 5 replicates.

RESULTS AND DISCUSSION

As a general strategy,[35] ROMP-based PNPs were assembled from short amphiphilic block copolymers consisting of one hydrophobic doxorubicin-conjugated block and a hydrophilic carboxy-terminated, poly(ethylene oxide) (PEO)-loaded block (Figure 1). With this design, the doxorubicin-loaded block constitutes the core of the PNPs, and the PEO-loaded segment forms a shell with terminal carboxy groups that can be used for further surface modification. The doxorubicin payload was linked to the hydrophobic segment through an acid-cleavable linkage,[4] which can be released in the low-pH environment of the late endosome[36] or in the tumor tissue.[37]

The amphiphilic block copolymers needed for PNP preparation were synthesized by block-copolymerizing the carboxy-terminated, PEO-conjugated monomer **2** and the doxorubicin-conjugated monomer **1** (Figure 1A). A 15:15 molar ratio for monomers **2:1** was chosen to

limit the molecular weight of the polymer < 45 kDa, thus facilitating renal clearance of the polymers post drug release.[38] Monomer **2** was successfully homo-polymerized using Grubbs' first-generation olefin metathesis ($(PCy_3)_2Cl_2Ru=CHPh$) catalyst (**3**) as confirmed by ^{1}H NMR spectroscopy and gel-permeation chromatography (GPC) analyses (M_n = 9000 (theoretical M_n = 8000), polydispersity index (PDI) = 1.17; Supporting Information (SI), Section S2). Sequential addition of monomer **1** to the homo-polymerized block **2**$_{15}$, followed by quenching with ethyl vinyl ether resulted in the formation of our desired monodisperse amphiphilic block copolymer **2**$_{15}$-*b*-**1**$_{15}$ (final polymer M_n = 15000 (theoretical M_n = 14000), PDI = 1.12; see Materials and Methods section and SI, Section S3).

Following our previously established strategy,[7] dropwise addition of water to a DMSO solution of copolymer **2**$_{15}$-*b*-**1**$_{15}$, followed by exhaustive dialysis against ultrapure deionized water, afforded an aqueous suspension of carboxy-functionalized, doxorubicin-loaded PNPs (Figure 1A). These nanoparticles have small hydrodynamic diameters (D_H = 63 ± 7 nm, Figure 1B) and exhibit a narrow size distribution (PDI = 0.11 ± 0.02), as measured by dynamic light scattering (DLS). Transmission electron microscopy (TEM) also confirmed their homogeneous spherical morphology (Figure 1C) with an average D_H of 65 ± 5 nm. Key to the realization of these small nanoparticle sizes was a fast rate of water addition over a shorter time period than previously reported[7] (see Materials and Methods section).

The covalent surface modification of the carboxy-functionalized PNPs with 3′-amine-terminated DNA was achieved using EDC/NHS coupling (Figure 1A). A mixture of the two components was stirred together with the EDC and NHS reagents for 4 h before being subjected to a salt-aging process to further increase the DNA density on the PNP surface[32] (see Materials and Methods section). After the total salt concentration reached 0.3 M, this mixture was allowed to react further overnight before being purified by size-exclusion chromatography. A TEM image (Figure 1D) of the isolated PSNA clearly shows the retention of the discrete and spherical morphology of the parent PNP (diameter ~ 87 nm). Their DLS-derived size distribution plot (Figure 1B) shows an increase in the hydrodynamic diameter (D_H = 88 ± 3 nm and PDI = 0.13 ± 0.03) that can be attributed to the addition of a dense DNA shell on the PNP surfaces. The shift in zeta potential (−5.1 ± 1.5 mV for the parent PNPs) to a higher negative value (−31.2 ± 3.2 mV for the PSNAs) also corroborates the successful conjugation of DNA to the PNP surface. Notably, the presence of the DNA shell on the surface of the PNP can be clearly observed upon staining of the PSNAs with uranyl acetate (z-contrast and transmission modes; Figure 1D). While not a primary focus of the current work, the thickness of the DNA shell can be changed by altering the length and composition of the oligonucleotide strands.[39] On average, ~1200 DNA strands/PNP were conjugated to the surface of each PNP as determined by fluorescence spectroscopy and nanoparticle tracking analysis (NTA) to quantify the number of PSNAs in a given sample via light scattering and Brownian motion. This DNA surface density (~7 pmol/cm^{2}, see Materials and Methods section for calculation) is comparable to but slightly higher than the loadings obtained for our previously reported liposomal SNA constructs.[40]

The doxorubicin-loaded PSNAs show excellent stability in comparison to the parent PNPs, a property that enables their use in cellular systems. For example, the PSNAs remain

colloidally stable after 2 months of incubation in phosphate-buffered saline (1× PBS) at room temperature (Figure 2A). In contrast, subjecting the unmodified PNPs to the same treatment for only a week resulted in formation of polydisperse aggregates irreversibly agglomerated, presumably through interparticle fusion. Most relevant for physiological applications, no change was observed in the DLS distribution plot for the PSNAs after 3 days of incubation at 37 °C in 1× PBS (Figures 2C and 2D). We attribute this enhanced stability to the electrostatic repulsion between the negatively charged oligonucleotides that comprise the shell of the PSNA, which inhibits particle-particle fusion under physiologically relevant conditions.[18] Notably, Dox-PSNAs remain stable in the presence of human serum while still maintaining their acid-triggered drug-release properties.[31] The doxorubicin-based fluorescence profiles for Dox-PSNAs after being incubated at 37 °C in PBS and human serum solution (10% v/v) are very similar as evidenced by minimal leakage of the drug (SI, Figure S8). In contrast, exposing Dox-PSNAs to 0.1 M HCl (aq) leads to a six-fold increase in drug release after one hour (SI, Figure S8).

Consistent with the assigned SNA structure, PSNAs cooperatively hybridize with complementary Au core SNAs. For example, when PSNAs were combined with complementary 13 nm Au-core SNAs (Figure 3A), visible aggregates can be observed and isolated. TEM analysis (Figures 3B and 3C) of these hybridized materials clearly shows a complete coverage of the larger PSNAs by the smaller Au-core SNAs. The increase in the melting temperature (T_m of the PNP-AuNP hybrid = 54.7 °C vs T_m = 52 °C (as calculated at 150 mM NaCl and 1.5 uM oligonucleotides using IDT OligoAnalyzer[41]) for the free DNA duplex analog) of these aggregates and their narrow thermal denaturation profile (full width at half-maximum (fwhm) of the first derivative is ~2.3 °C) confirms cooperative binding behavior that is characteristic of SNAs[15] (Figure 3D).

As expected, the dense oligonucleotide shell of the Dox-PSNAs greatly facilitates their entrance into cells. As shown by confocal microscopy, SKOV-3 cells (ovarian cancer ascites) readily uptake Dox-PSNAs that were surface-modified with 5′-Cy5-labelled oligonucleotides (Figure 4A). This is in stark contrast to the non-functionalized PNP analog, which settles out of cell culture media due to aggregation and shows low and non-uniform uptake.[31] Such enhanced cellular internalization of SNA structures has been attributed by Mirkin and coworkers to the interaction of the oligonucleotide shell with Class A scavenger receptors (SR-A) present on the cell surface, followed by caveolin-mediated endocytosis.[23] Because our goal was to enhance the delivery of the therapeutically active payload of Dox-PSNAs to diseased cells, a generic T_{20} DNA sequence was sufficient for this purpose. We note in passing that although a detailed mechanistic study comprising competitive and endocytosis inhibition assays can be carried out to ascertain the exact uptake mechanism, such a study is beyond the scope of the present work.

The cellular internalization properties of the Dox-loaded PSNAs (Dox-PSNAs) lead to *in-vitro* cytotoxicity against SKOV3 cancer cells that is comparable to that of free doxorubicin (Figure 4B). Such a study could not have been properly carried out with the parent PNPs due to their aggregation behavior in biological media. Indeed, PNPs have been observed to settle out of cell culture media over time, leading to low and non-uniform uptake in SKNSH wild-type cells.[31] The observed cytotoxicity of the Dox-PSNAs can be attributed to the acid-

induced cleavage of the carbamate linkage between the block copolymer backbone and the doxorubicin, allowing for the release of the latter into the cytoplasm.[6,31] Supporting this conclusion is the observation that the analogous PSNAs with cholesterol-loaded cores does not show any cytotoxicity against SKOV3 cells (SI, Section S5).

CONCLUSIONS

In summary, we have demonstrated that the successful modification of doxorubicin-loaded PNPs with a dense oligonucleotide shell greatly increases their colloidal stability in biological media under physiological conditions. The dense shell of oligonucleotides allows the resulting Dox-PSNAs to have enhanced cellular uptake, manifesting in cytotoxicity that is comparable to the free drug. Importantly, this SNA-based strategy should be generalizable to other therapeutic-loaded nanoparticles for *in vivo* applications in the treatment of cancer and other diseases.

Supplementary Material

Refer to Web version on PubMed Central for supplementary material.

Acknowledgments

ABBREVIATIONS

Dox	doxorubicin
D_H	hydrodynamic diameters
DLS	dynamic light scattering
NTA	nanoparticle tracking analysis
PDI	polydispersity index
PEG	poly(ethylene glycol)
PNP	polymeric nanoparticles
PSNA	polymeric spherical nucleic acids
ROMP	ring-opening metathesis polymerization

References

1. Rush AM, Nelles DA, Blum AP, Barnhill SA, Tatro ET, Yeo GW, Gianneschi NC. J Am Chem Soc. 2014; 136:7615–7618. [PubMed: 24827740]

2. Bertin PA, Gibbs JM, Shen CK, Thaxton CS, Russin WA, Mirkin CA, Nguyen ST. J Am Chem Soc. 2006; 128:4168–4169. [PubMed: 16568958]

3. Allen MJ, Raines RT, Kiessling LL. J Am Chem Soc. 2006; 128:6534–6535. [PubMed: 16704234]

4. Bertin PA, Smith D, Nguyen ST. Chem Commun. 2005; 41:3793–3795.

5. Callmann CE, Barback CV, Thompson MP, Hall DJ, Mattrey RF, Gianneschi NC. Adv Mater. 2015; 27:4611–4615. [PubMed: 26178920]

6. Krovi SA, Smith D, Nguyen ST. Chem Commun. 2010; 46:5277–5279.

7. Krovi SA, Swindell EP, O'Halloran TV, Nguyen ST. J Mater Chem. 2012; 22:25463–25470. [PubMed: 23509417]

8. Mukherjee S, Patra D, Dinda H, Chalkraborty I, Shashank L, Bhattacharyya R, Das Sarma J, Shunmugam R. Macromolecules. 2016; 49:2411–2418.

9. Huang K, Ma H, Liu J, Huo S, Kumar A, Wei T, Zhang X, Jin S, Gan Y, Wang PC, He S, Zhang X, Liang XJ. ACS Nano. 2012; 6:4483–4493. [PubMed: 22540892]

10. Choi JS, Cao J, Naeem M, Noh J, Hasan N, Choi HK, Yoo JW. Colloids Surf, B. 2014; 122:545–551.

11. Tang L, Gabrielson NP, Uckun FM, Fan TM, Cheng J. Mol Pharmaceutics. 2013; 10:883–892.

12. Cutler JI, Auyeung E, Mirkin CA. J Am Chem Soc. 2012; 134:1376–1391. [PubMed: 22229439]

13. Cabral H, Matsumoto Y, Mizuno K, Chen Q, Murakami M, Kimura M, Terada Y, Kano MR, Miyazono K, Uesaka M, Nishiyama N, Kataoka K. Nat Nanotechnol. 2011; 6:815–823. [PubMed: 22020122]

14. Biondi M, Guarnieri D, Yu H, Belli V, Netti PA. Nanotechnology. 2013; 24:045101. [PubMed: 23293277]

15. Mirkin CA, Letsinger RL, Mucic RC, Storhoff JJ. Nature. 1996; 382:607–609. [PubMed: 8757129]

16. Lee JS, Lytton-Jean AK, Hurst SJ, Mirkin CA. Nano Lett. 2007; 7:2112–2115. [PubMed: 17571909]

17. Young KL, Scott AW, Hao L, Mirkin SE, Liu G, Mirkin CA. Nano Lett. 2012; 12:3867–3871. [PubMed: 22725653]

18. Banga RJ, Chernyak N, Narayan SP, Nguyen ST, Mirkin CA. J Am Chem Soc. 2014; 136:9866–9869. [PubMed: 24983505]

19. Brodin JD, Auyeung E, Mirkin CA. Proc Natl Acad Sci U S A. 2015; 112:4564–4569. [PubMed: 25831510]

20. Peterson AM, Heemstra JM. Wiley Interdiscip Rev: Nanomed Nanobiotechnol. 2015; 7:282–297. [PubMed: 25327363]

21. Jia F, Lu X, Tan X, Zhang K. Chem Commun. 2015; 51:7843–7846.

22. Giljohann DA, Seferos DS, Patel PC, Millstone JE, Rosi NL, Mirkin CA. Nano Lett. 2007; 7:3818–3821. [PubMed: 17997588]

23. Choi CH, Hao L, Narayan SP, Auyeung E, Mirkin CA. Proc Natl Acad Sci U S A. 2013; 110:7625–7630. [PubMed: 23613589]

24. Wu XA, Choi CH, Zhang C, Hao L, Mirkin CA. J Am Chem Soc. 2014; 136:7726–7733. [PubMed: 24841494]

25. Giljohann DA, Seferos DS, Prigodich AE, Patel PC, Mirkin CA. J Am Chem Soc. 2009; 131:2072–2073. [PubMed: 19170493]

26. Dhar S, Daniel WL, Giljohann DA, Mirkin CA, Lippard SJ. J Am Chem Soc. 2009; 131:14652–+. [PubMed: 19778015]

27. Tan X, Li BB, Lu X, Jia F, Santori C, Menon P, Li H, Zhang B, Zhao JJ, Zhang K. J Am Chem Soc. 2015; 137:6112–6115. [PubMed: 25924099]

28. Tan XY, Lu XG, Jia F, Liu XF, Sun YH, Logan JK, Zhang K. J Am Chem Soc. 2016; 138:10834–10837. [PubMed: 27522867]

29. Radovic-Moreno AF, Chernyak N, Mader CC, Nallagatla S, Kang RS, Hao L, Walker DA, Halo TL, Merkel TJ, Rische CH, Anantatmula S, Burkhart M, Mirkin CA, Gryaznov SM. Proc Natl Acad Sci U S A. 2015; 112:3892–3897. [PubMed: 25775582]

30. Kadam RS, Bourne DWA, Kompella UB. Drug Metab Dispos. 2012; 40:1380–1388. [PubMed: 22498894]

31. Smith D, Clark SH, Bertin PA, Mirkin BL, Nguyen ST. J Mater Chem. 2009; 19:2159–2165. [PubMed: 24421587]

32. Hurst SJ, Lytton-Jean AK, Mirkin CA. Anal Chem. 2006; 78:8313–8318. [PubMed: 17165821]

33. Li HL, Sun XP. Chem Commun. 2011; 47:2625–2627.

34. Wang L, Zhang Y, Tian J, Li H, Sun X. Nucleic Acids Res. 2011; 39:e37. [PubMed: 21183465]

35. Bertin PA, Watson KJ, Nguyen ST. Macromolecules. 2004; 37:8364–8372.

36. Deng X, Wang Y, Zhang F, Yin Z, Hu Q, Xiao X, Zhou Z, Wu Y, Sheng W, Zeng Y. Chem Commun. 2016; 52:3243–3246.

37. Poon Z, Chang D, Zhao X, Hammond PT. ACS Nano. 2011; 5:4284–4292. [PubMed: 21513353]

38. Nori A, Kope ek J. Adv Drug Delivery Rev. 2005; 57:609–636.

39. Narayan SP, Choi CH, Hao L, Calabrese CM, Auyeung E, Zhang C, Goor OJ, Mirkin CA. Small. 2015; 11:4173–4182. [PubMed: 26097111]

40. Hill HD, Millstone JE, Banholzer MJ, Mirkin CA. ACS Nano. 2009; 3:418–424. [PubMed: 19236080]

41. https://www.idtdna.com/calc/analyzer; accessed on April 2, 2016.

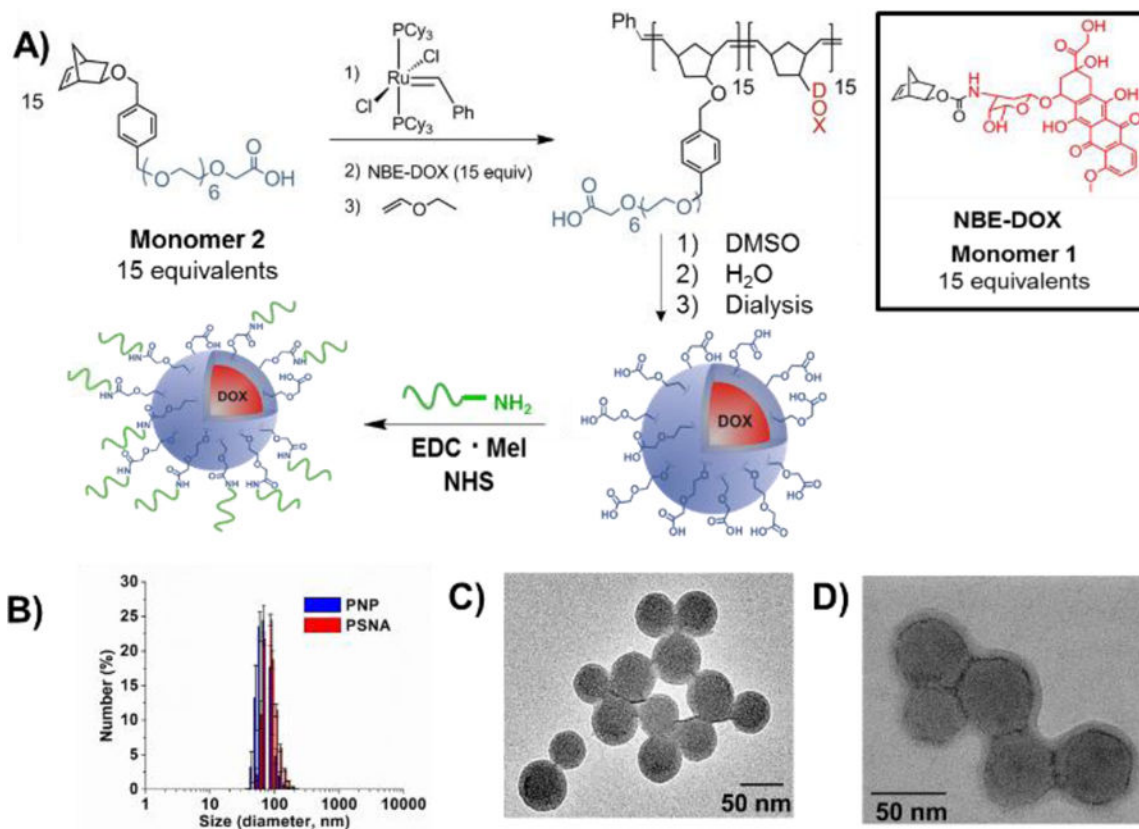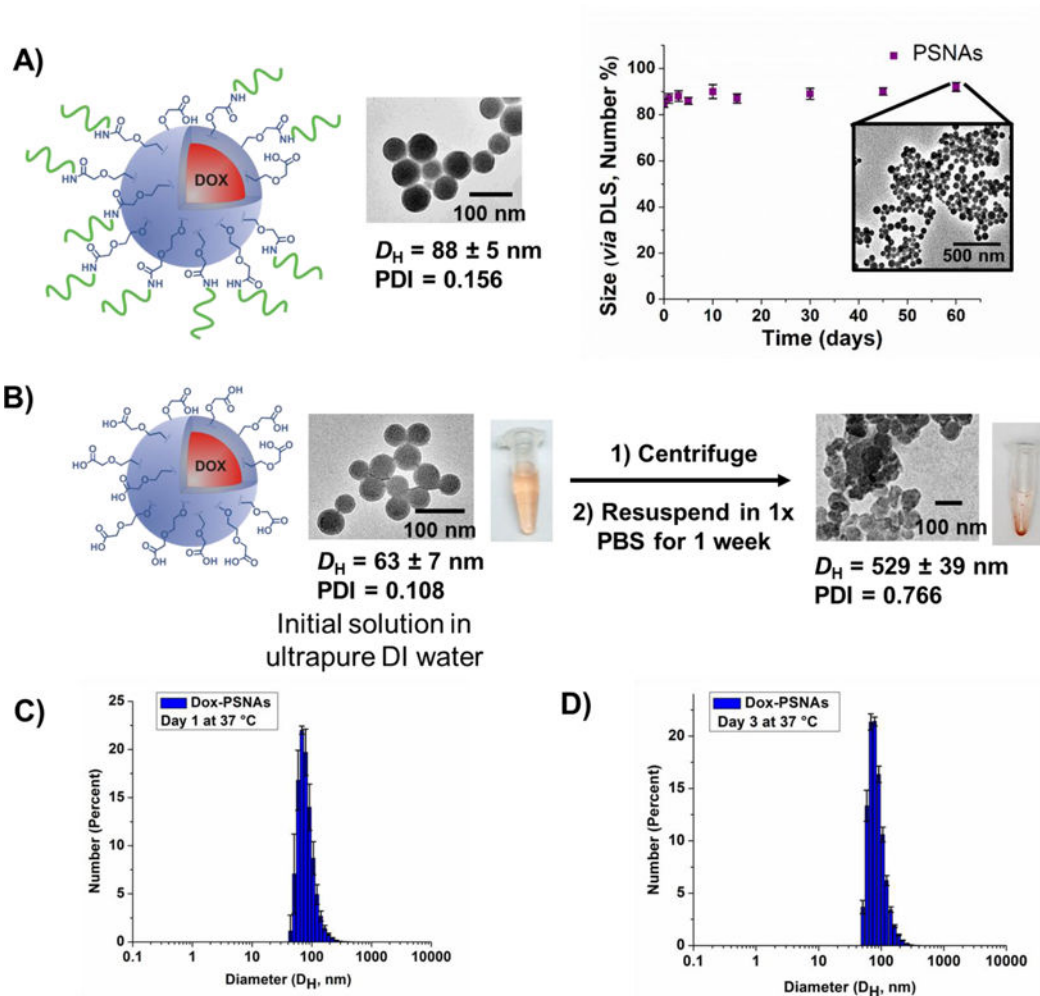42. Lee S-M, Chen H, O'Halloran TV, Nguyen ST. J Am Chem Soc. 2009; 131:9311–9320. [PubMed: 19527027]

Figure 1.
A) Synthesis of block copolymer **1**$_{15}$-*b*-**2**$_{15}$ and subsequent formation of the corresponding PNPs. B) Dynamic light scattering (DLS) data for the PNPs before and after covalent DNA functionalization. C–D) TEM image of the PNPs before (C) and after (D) DNA functionalization.

Figure 2.
A) Doxorubicin-loaded PSNAs remain stable for over two months in 1× PBS as analysed by TEM and DLS. B) Doxorubicin-loaded PNPs aggregate when incubated in 1× PBS for a week. C and D) DLS profiles for Dox-PSNAs confirming their stablity in 1× PBS at 37 °C for 3 days.
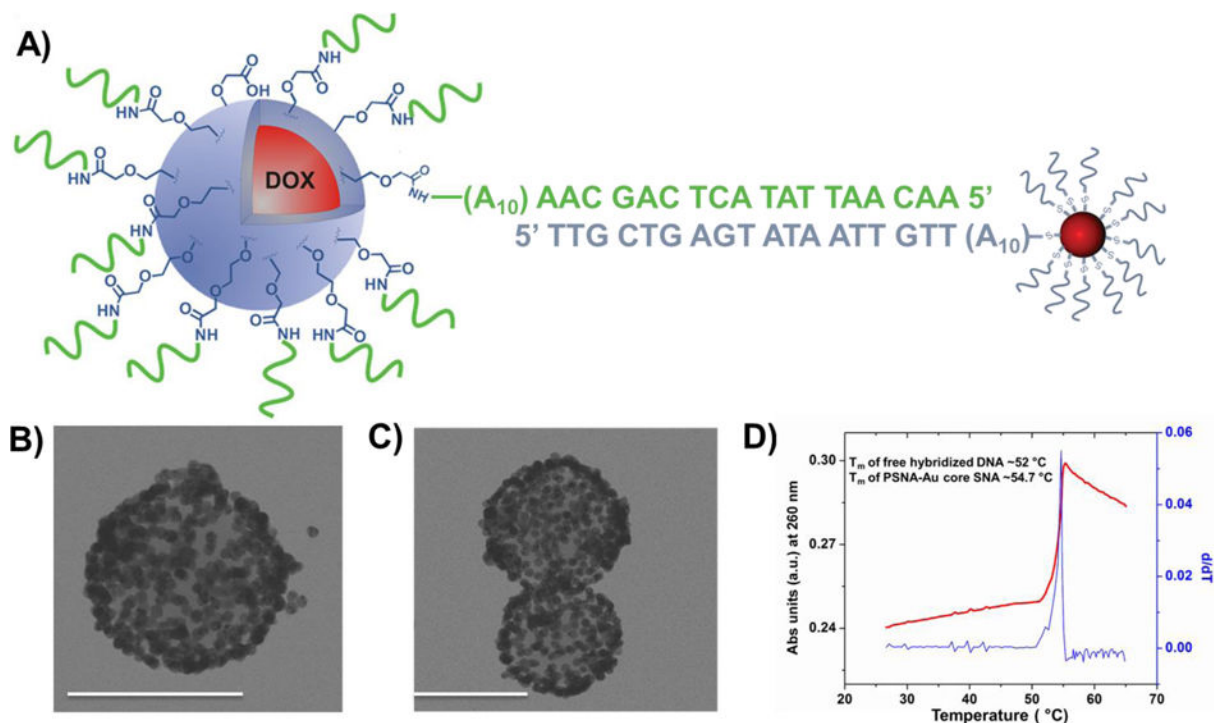
Figure 3.
A) A schematic drawing of the Dox-PSNAs hybridized to complementary 13 nm Au-core SNAs. B–C) TEM images of the Dox-PSNAs surrounded by complementary Au-core SNAs conjugates. Scale bar is 100 nm. D) The thermal denaturation profile (red) of the [Dox-PSNAs + Au-core SNAs] hybridized aggregates monitored as a change in extinction at 260 nm. The overlaid 1st derivative (blue) of this profile shows the sharp melting transition. See SI, section S10 for the control experiment.
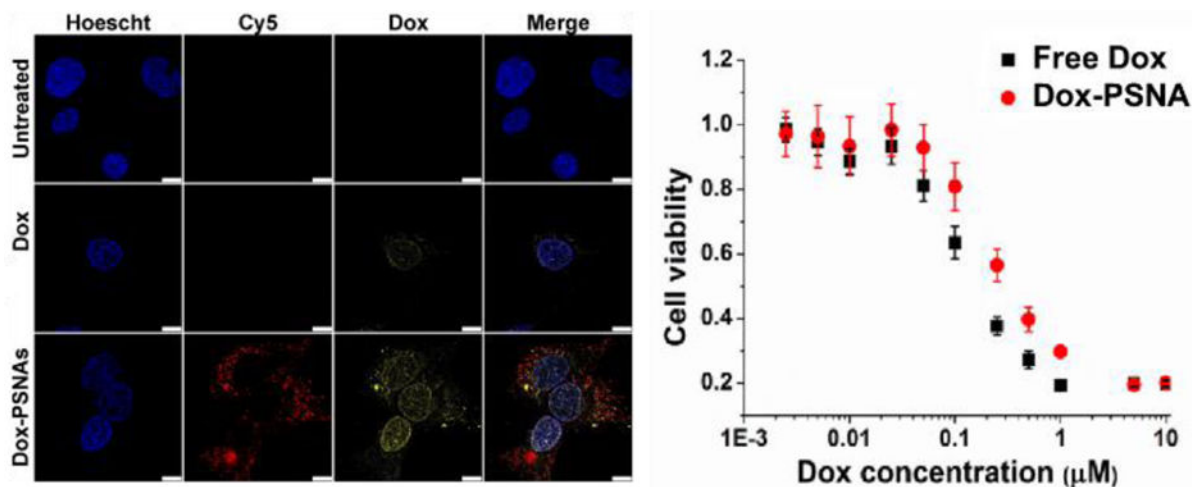
Figure 4.
A) Confocal laser-scanning microscopy images of SKOV-3 cells that have been incubated for 24 h with free doxorubicin (Dox) and doxorubicin-loaded PSNAs (Dox-PSNAs) at 2.5 µM Dox concentration. Given the qualitative nature of the confocal image (e.g., change in focal point between sample wells), the various signal intensities should not be compared across rows. In addition, each panel is limited to a few cells and do not represent the entire population. A statistically significant flow cytometry study (SI, Figure S10) does show higher doxorubicin fluorescence signal for the cells that have been incubated with free doxorubicin. B) Cytotoxicity profiles for SKOV-3 cells that have been incubated for 48 h with dox and Dox-PSNA formulations at 5 nM-10 µM [Dox]. The similarity in toxicity between the doxorubicin-loaded NPs and free doxorubicin is not surprising given previous studies from our group,[31,42] and the fact that IC_{50} measurements are highly dependent on many variables (treatment time, incubation time post-treatment, release of payload from the delivery vehicle, cell type and confluency) and can vary by several fold, depending on conditions.
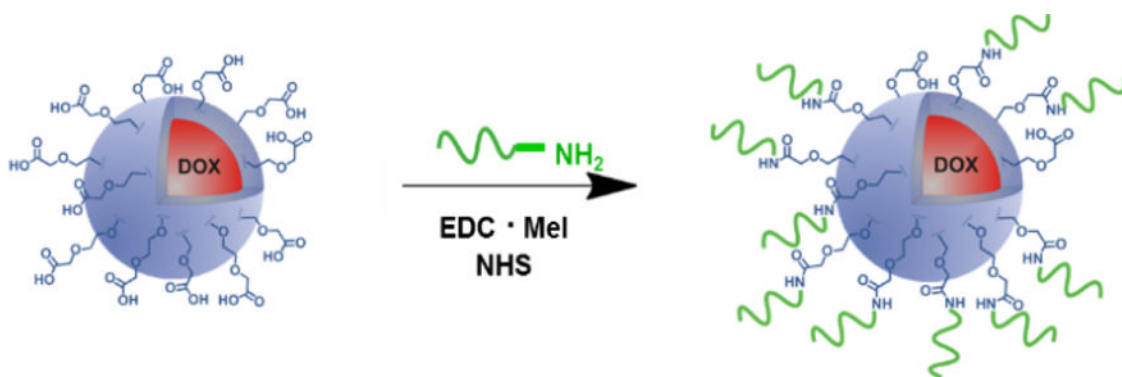
Scheme 1.
The covalent surface modification of carboxy-functionalized PNPs with amine-terminated oligonucleotides (green) via amide-coupling chemistry.